

Colored Conical Emission by Means of Second Harmonic Generation in a Quadratically Nonlinear Medium

Heping Zeng, Jian Wu, Han Xu, Kun Wu, and E Wu

Key Laboratory of Optical and Magnetic Resonance Spectroscopy, and Department of Physics, East China Normal University, Shanghai 200062, People's Republic of China

(Received 29 August 2003; revised manuscript received 9 December 2003; published 8 April 2004)

Colored conical emission was observed experimentally in a thick β -barium borate crystal as a result of spatiotemporal modulational instability. In the presence of both dispersion and diffraction, colored conical emission showed specific features that were characteristic of the nonlinear dynamics of the strongly coupled fundamental and harmonic fields. Experimental observation directly demonstrated that beam angular spectra were substantially modified as a result of exponential growth of perturbations by means of parametric wave mixing. Seeded amplification of colored conical emission was demonstrated to support ultrabroadband up-conversion.

DOI: 10.1103/PhysRevLett.92.143903

PACS numbers: 42.65.Sf, 03.50.De, 42.65.Jx, 42.65.Tg

In the optical domain, modulational instability (MI) occurs during light propagation in a nonlinear medium due to the interplay of optical Kerr nonlinearity and group velocity dispersion or diffraction, which causes exponential growth of perturbations either in time as temporal breakup [1] or in space as filamentation [2–4], respectively. In a quadratically nonlinear medium, MIs occur during the second harmonic generation due to the parametric instability [5–8]. The dynamic interaction of the strongly coupled fundamental and harmonic fields was observed to induce breakup of highly elliptical input beams into a line of circular separated beams as quadratic spatial solitons [5]. Spatiotemporal instability occurs in the presence of both diffraction and dispersion that act together to couple space and time [9–11]. Recent experimental observations on self-focusing behaviors of intense ultrashort pulses indicated that spatial and temporal degrees of freedom could not be treated separately [10]. Interestingly, in a nonlinear medium when diffraction, group velocity dispersion, and nonlinearity have comparable characteristic length scales, space-time coupling may originate in the formation of a nondiffracting and nondispersive localized wave packet, i.e., a spatiotemporal soliton or light bullet [10]. Spatiotemporal MIs in quadratic bulk samples were predicted to cause exponential growth of perturbations which result in colored conical emission [11]. In pertinent experiments, conical emissions (CEs) have been observed with near-resonance pulse propagation in dense metal vapors [12,13], and ultrashort pulse filamentation in air [14–19].

In this Letter, we report on the experimental observation of CEs and seeded amplification of conical emission (SAC) in a thick β -barium borate (BBO) crystal pumped by intense fs pulses from a Ti:sapphire laser. Bright colored cones around the second harmonic wave were observed and their characteristics were investigated in detail. SAC was demonstrated to withstand the presence of group velocity mismatch (GVM) in a thick nonlinear

crystal, yielding what we believe to be the highest tunable fs up-conversion to date, which showed a promising prospect for ultrabroadband parametric amplification to achieve intense fs pulses. This was quite different from the traditional optical parametric amplification, where thin nonlinear crystals are usually used in order to minimize temporal walk-offs between the interacting ultrashort pulses [20–23]. Moreover, SAC supported up-conversion under the infrared fs pump, while only down-converted signal and idler photons can be generated in the traditional optical parametric amplification. Up-conversion itself implied that there occurred multiple three-photon parametric wave-mixing processes in the quadratic medium.

In the experiments, we used a 1 kHz regeneratively amplified Ti:sapphire fs laser (Spitfire, Spectra-Physics) to obtain fs pulses with the single-pulse energy of about 650 μ J. The laser beam was focused by a concave high-reflection mirror with a focus length of 100 cm. A 6-mm-thick β -BBO crystal (type-I, 29.18° cut) was placed before the focus. As shown in Fig. 1(a), an iris was placed before the concave mirror to vary the diameter and divergent angle of the laser beam focused into the crystal, and to change the incident fluence of the fundamental pulse as well. As the fundamental pulse reached a sufficient intensity and the β -BBO crystal was rotated to maximize the second harmonic generation, a bright blue-green cone with a conical angle of $\theta \sim 5.0^\circ$ emerged around the propagation axis as shown in Figs. 1(b)–1(d). The blue-green CE approximately peaked near 500 nm, which exhibited an angular width of about 0.4° (4.77° – 5.17°). As the chirp or beam divergence of the fundamental pulses was changed, CE changed accordingly. When the iris was changed to a smaller diameter, the blue-green CE became less intense, and a red semi-conical emission appeared inside the blue-green CE with an asymmetric spatial distribution around the propagation axis. A typical image and the corresponding

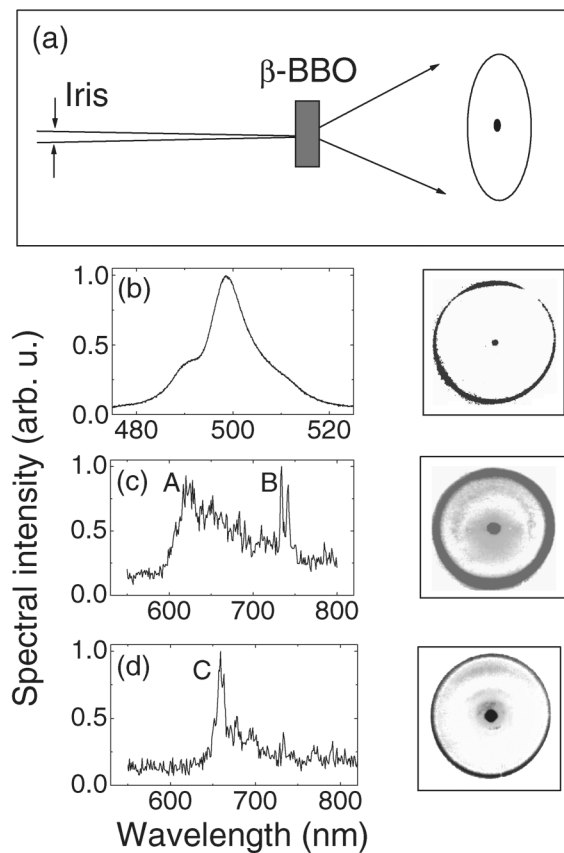


FIG. 1. (a) Schematic of the experimental setup. (b) Bright blue-green CE and the corresponding spectra observed at the optimum chirp and angular spectra of the fundamental pulses. (c) CE rings observed with the fundamental pulses passing through a smaller iris, and typical spectra of the red semiconical emission. (d) CE rings excited by a negatively chirped fundamental pulse, and typical spectra of the red semiconical emission.

spectrum of the red CE are given in Fig. 1(c). When small negative chirps were intentionally introduced to the fundamental pulses, red semiconical emissions also appeared within the weakened blue-green CEs. A typical CE ring and the corresponding emission spectrum are given in Fig. 1(d). Since the changes of the pulse chirp and iris diameter were, respectively, equivalent to the changes of the temporal and spatial modes of the fundamental pulses, the above observations indicated that space played the same role as time to entail CEs [11].

To demonstrate that the observed CEs were originated from strong coupling between the fundamental and second harmonic pulses, we rotated the β -BBO crystal to change second harmonic conversion while we kept the fundamental pulses unchanged. Figure 2(a) gives the dependence of the blue-green CE pulse energy upon the rotation angle of crystal. This clearly indicated that the observed CEs were originated from coupling between the fundamental and second harmonic pulses. As mentioned above, the blue-green CEs became weak when the fundamental pulses were chirped to produce long

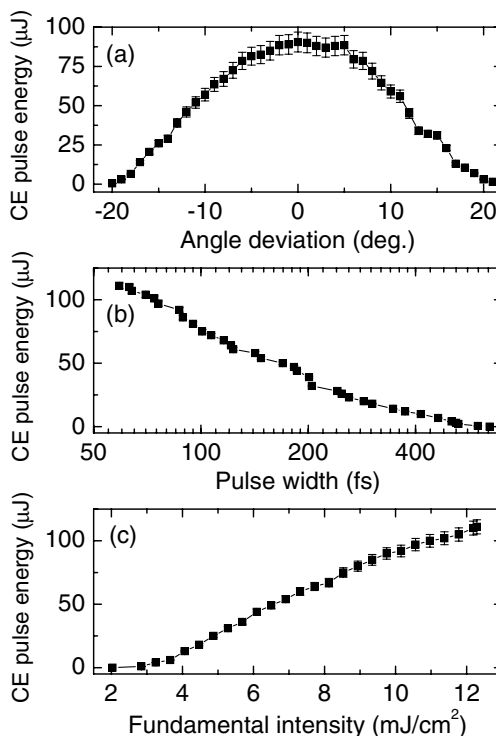


FIG. 2. The dependence of the pulse energy of the blue-green CE upon (a) the rotation of the β -BBO crystal with the angle deviated from its optimum for maximum blue-green CE, (b) the pulse width of the fundamental pulses, and (c) the fundamental intensity.

pulses. As shown in Fig. 2(b), the dependence of the blue-green CE pulse energy upon the fundamental pulse widths was approximately reciprocal at long pulses and slightly deviated to the reciprocal dependence at short pulses. The blue-green CE pulse energies were also measured at different fundamental laser intensities by using a variable attenuator. As shown in Fig. 2(c), blue-green CE was clearly observed under a 60-fs fundamental pump when the intensity reached a value about 3.0 mJ/cm^2 , above which the CE pulse energy increased monotonously with the fundamental pump intensity. As shown in Fig. 3, the spectrum of the bright blue-green CE also changed with the fundamental chirp, and different CE spectra were observed under different pump intensities, where the pump intensity was changed by using a variable attenuator or by scanning the β -BBO crystal along the slightly focused fundamental beam. Note that the spatial and temporal modes of the fundamental pulses were maintained during the variation of pump intensities. These phenomena clearly indicated that the observed CEs were originated from strong spatiotemporal coupling between the fundamental and second harmonic pulses [1,6,11].

When seeded with an accurately synchronized white supercontinuum (WS), CEs caused the injected seed to grow exponentially. The WS pulses, which were generated from a 2-mm-thick sapphire plate pumped by a

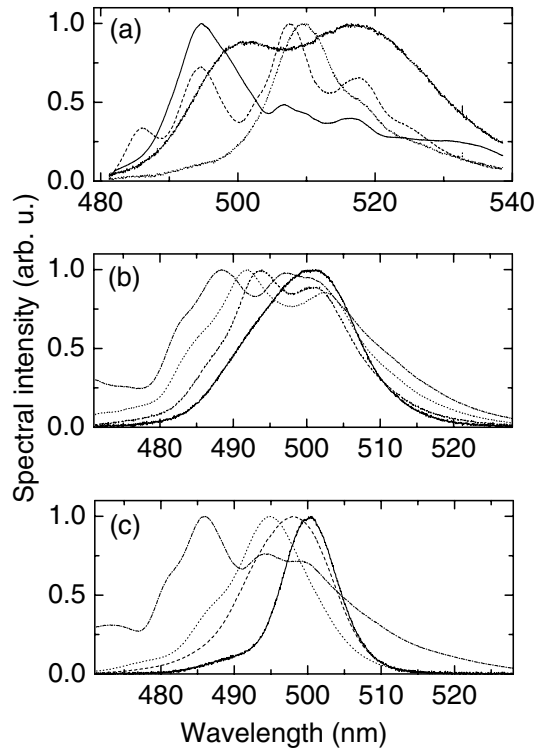


FIG. 3. The spectra of the bright blue-green CE (a) pumped by negatively chirped fundamental pulses with the FWHM duration of 78 fs (solid line), 176 fs (dashed line), 342 fs (dotted line), and 464 fs (dash-dotted line), (b) pumped by fundamental pulses (78 fs) after a variable attenuator to get variable intensities at 3.8 mJ/cm² (solid line), 5.5 mJ/cm² (dashed line), 8.9 mJ/cm² (dotted line), and 12.0 mJ/cm² (dash-dotted line), and (c) pumped by slightly focused fundamental pulses (78 fs) with the β -BBO crystal being scanning to get variable intensities at 8.3 mJ/cm² (solid line), 9.2 mJ/cm² (dashed line), 10.1 mJ/cm² (dotted line), and 11.9 mJ/cm² (dash-dotted line), respectively.

split fraction (6%) from the fundamental pulses, were collimated into the β -BBO crystal along the conical angle of the blue-green CE ($\theta = 5.0^\circ$). When the delay between the seed and fundamental pulses was adjusted to get accurate synchronization, SAC produced a sparkling pearl on the blue-green CE, as labeled by point A in the inset of Fig. 4(a). The output beam had a typical picture and beam profile as shown in Fig. 4(b). SAC generated broadband pulses with much broader full width at half maximum (FWHM) than the blue-green CE (~ 10 nm). Figure 4(a) presents a typical SAC spectrum with the FWHM up to 64 nm. As shown in Fig. 4(c), the SAC output pulse energy increased monotonously with the fundamental intensity and reached 150 μ J at the fundamental intensity of 13.9 mJ/cm². This was more than 1 order of magnitude higher than those obtained with comparable fundamental lasers by using standard optical parametric amplification [20–23]. A stability test of the SAC output pulses, as shown in Fig. 4(d) for a typical operation within 15 min, indicated that the SAC output

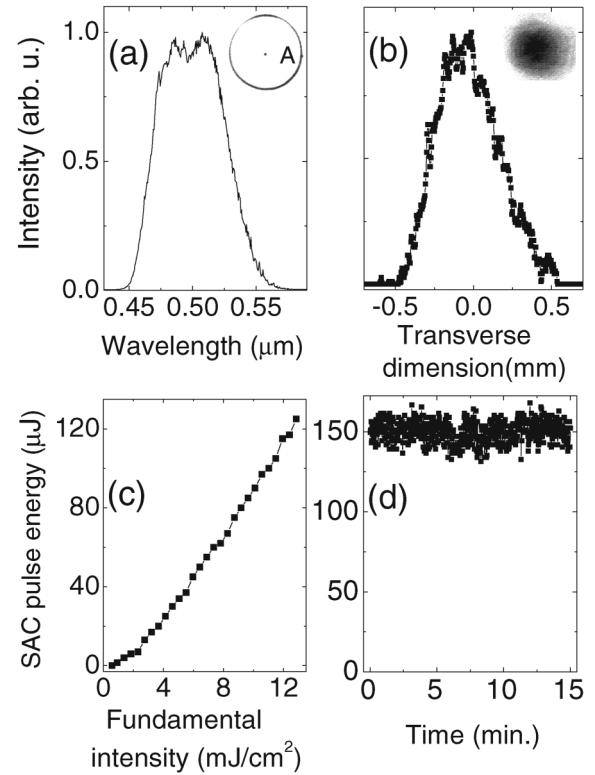


FIG. 4. (a) SAC spectra near 500 nm and the corresponding picture given in the inset, (b) the spatial distribution of SAC output near 500 nm and the transverse profile given in the inset, (c) dependence of the SAC output pulse energy with the fundamental pump intensity, and (d) stability of SAC output pulse energy.

pulses were stable with a standard deviation of 4.5%. The M^2 parameter of the SAC output beam was measured to be 5.4 at a typical operation with the output energy of 100 μ J under the fundamental pump of 12 mJ/cm².

Intrinsically, CE by means of second harmonic generation involved multiple three-photon processes [11]. As pumped by on-axis pulses at the fundamental frequency ω and the associated second harmonic frequency 2ω , spatiotemporal MIs induced decay of second harmonic photons into photon pairs at shifted frequencies $\omega_{\pm} = \omega \pm \delta$ traveling with opposite off-axis angles [11], determined by the noncollinear phase matching $\vec{k}(2\omega) = \vec{k}(\omega_+) + \vec{k}(\omega_-)$, which gives k_t for the transverse projection of $\vec{k}(\omega_+)$ as

$$k_t^2 = k^2(\omega_+) - \frac{[k^2(2\omega) + k^2(\omega_+) - k^2(\omega_-)]^2}{4k^2(2\omega)}, \quad (1)$$

where δ is the frequency shifted away from the fundamental frequency ω . The conical angle of the CE is given by $\sin\theta = k_t/k(\omega_+)$, from which we calculated that the blue-green CE had a conical angle $\theta = 5.0^\circ$ in air. Inside the blue-green cone, CEs occurred in the region between 500 and 800 nm. Accordingly, SAC occurred in the same range as the WS pulses were seeded along conical angles $\theta \leq 5.0^\circ$. The angular dependence of the CE

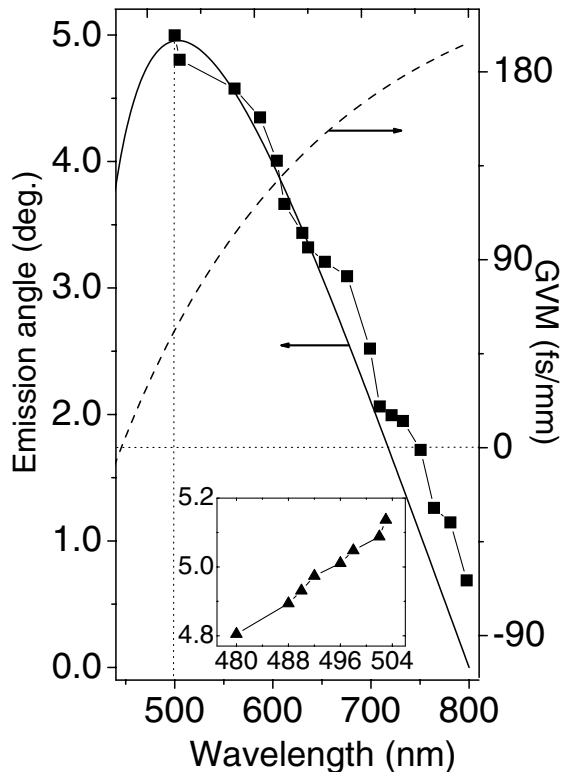


FIG. 5. Angular dependence of CE measured by tuning SAC at different seeding angles of the WS pulses, calculated CE angles at different wavelengths, and calculated GVM between the on-axis second harmonic and off-axis CE pulses. The inset is the angularly resolved spectral centers of the blue-green CE.

spectra could thus be measured by tuning SAC at different seeding angles of the WS pulses. Figure 5 presents the output wavelength tuning curve of SAC at the correspondingly optimized synchronization when the seeding angle of the WS pulses was adjusted from $\theta = 5.0^\circ$ to $\theta = 0.68^\circ$. For comparison, we present in the inset the angularly resolved spectral centers of the blue-green CE near $\theta = 5.0^\circ$. Clearly, the angular dependence of the CE central wavelength changed near the blue-green CE at $\theta = 5.0^\circ$. This can be qualitatively understood from the phase-matching curve calculated from Eq. (1), which indicates that there exists a maximum phase-matching angle near 500 nm ($\theta \sim 5.0^\circ$). According to the calculated GVM between on-axis second harmonic and off-axis CE pulses, the minimum GVM locates at 475 nm, which has a phase-matching angle $\theta \sim 4.8^\circ$, while the strongest CE occurred at 500 nm with the conical angle $\theta = 5.0^\circ$, where the corresponding GVM is about 29.4 fs/mm. Interestingly, SAC withstood the presence of GVM even for a broadband seed injection in a thick nonlinear crystal.

In summary, we have experimentally observed conical emissions by means of second harmonic generation and seeded amplification of conical emission in a thick β -barium borate crystal. SAC was demonstrated to support significant amplification of up-converted pulses

under the infrared pump, which can be used as a novel technique for ultrabroadband parametric amplification to generate tunable intense ultrashort pulses.

This work was supported by Shanghai Priority Academic Discipline, by National Key Project for Basic Research (No. TG1999075204), and by National Natural Science Foundation (No. 10234030).

- [1] K. Tai, A. Hasegawa, and A. Tomita, *Phys. Rev. Lett.* **56**, 135 (1996).
- [2] R. Malendevich, L. Jankovic, G. Stegeman, and J.S. Aitchison, *Opt. Lett.* **26**, 1879 (2001).
- [3] For an early review, see A.A. Akhmanov, R.V. Khokhlov, and A.P. Sukhorukov, *Laser Handbook*, edited by F.T. Arecchi and E.O. Schulz-Dubois (North-Holland, Amsterdam, 1972), pp. 1151–1228.
- [4] A. Braun, G. Korn, X. Liu, D. Du, J. Squier, and G. Mourou, *Opt. Lett.* **20**, 73 (1995).
- [5] R.A. Fuerst, D.-M. Baboiu, B. Lawrence, W.E. Torruellas, G.I. Stegeman, S. Trillo, and S. Wabnitz, *Phys. Rev. Lett.* **78**, 2756 (1997).
- [6] R. Schiek, H. Fang, R. Malendevich, and G.I. Stegeman, *Phys. Rev. Lett.* **86**, 4528 (2001).
- [7] S. Trillo and P. Ferro, *Opt. Lett.* **20**, 438 (1995).
- [8] S. Trillo and S. Wabnitz, *Phys. Rev. E* **55**, R4897 (1997).
- [9] C. Conti, *Phys. Rev. E* **68**, 016606 (2003).
- [10] C. Conti, S. Trillo, P. Di Trapani, G. Valiulis, A. Piskarskas, O. Jedrkiewicz, and J. Trull, *Phys. Rev. Lett.* **90**, 170406 (2003).
- [11] S. Trillo, C. Conti, P. Di Trapani, O. Jedrkiewicz, J. Trull, G. Valiulis, and G. Bellanca, *Opt. Lett.* **27**, 1451 (2002).
- [12] W. Chalupczak, W. Gawlik, and J. Zachorowski, *Phys. Rev. A* **49**, R2227 (1994).
- [13] W.K. Lee, Y.C. Noh, J.H. Jeon, J.H. Lee, J.S. Chang, K.H. Ko, and J. Lee, *J. Opt. Soc. Am. B* **18**, 101 (2001).
- [14] J. Yu, D. Mondelain, G. Ange, R. Volk, S. Niedermeier, J.P. Wolf, J. Kasparian, and R. Sauerbrey, *Opt. Lett.* **26**, 533 (2001).
- [15] E.T.J. Nibbering, P.F. Curley, G. Grillon, B.S. Prade, M.A. Franco, F. Salin, and A. Mysyrowicz, *Opt. Lett.* **21**, 62 (1996).
- [16] O.G. Kosareva, V.P. Kandidov, A. Brodeur, C.Y. Chien, and S.L. Chin, *Opt. Lett.* **22**, 1332 (1997).
- [17] S. Tzortzakis, L. Bergé, A. Couairon, M. Franco, B. Prade, and A. Mysyrowicz, *Phys. Rev. Lett.* **86**, 5470 (2001).
- [18] A. Couairon and L. Bergé, *Phys. Rev. Lett.* **88**, 135003 (2002).
- [19] N. Akozbek, A. Iwasaki, A. Becker, M. Scalora, S.L. Chin, and C.M. Bowden, *Phys. Rev. Lett.* **89**, 143901 (2002).
- [20] T. Whithelm, J. Piel, and E. Riedle, *Opt. Lett.* **22**, 1494 (1997).
- [21] A. Shirakawa and T. Kobayashi, *Appl. Phys. Lett.* **72**, 147 (1998).
- [22] A. Baltuška, T. Fuji, and T. Kobayashi, *Opt. Lett.* **27**, 306 (2002).
- [23] P. Tzankov, T. Fiebig, and I. Buchvarov, *Appl. Phys. Lett.* **82**, 517 (2003).